J Aust Ceram Soc (2018) 54:205–214
DOI 10.1007/s41779-017-0142-7

RESEARCH

Effect of abrasive waterjet machining on $LaPO_4/Y_2O_3$ ceramic matrix composite

K. Balamurugan[1] · **M. Uthayakumar**[2] · **S. Sankar**[3] · **U. S. Hareesh**[3] · **K. G. K. Warrier**[3]

Received: 21 January 2017 / Revised: 24 August 2017 / Accepted: 8 September 2017 / Published online: 18 September 2017

Abstract $LaPO_4/Y_2O_3$ composite is identified as potential materials that possess low thermal conductivity and superior hardness and finds its application as high thermal barrier material and also a functional material. The objective of the study is to exhibit the correlation of three independent parameters of AWJM on $LaPO_4/Y_2O_3$ composite prepared by Aqueous Sol-Gel process by response surface method (RSM). Jet pressure (JP), stand-off distance (SOD) and traverse speed (TS) are taken as the three independent parameters of AWJM. Effects of these parameters are measured and validated through three dependent responses of material removal rate (MRR), Kerf angle (KA) and surface roughness (Ra). To perform the experimental observations, central composite design (CCD) of L20 orthogonal array is used. Garnet of 80 meshes is used as abrasive. The microstructure of the cut region has plastic deformation surface with micro wear track and crack. Through RSM, it is identified that the three independent parameters have equal contributions on MRR and KA, where SOD has a significant effect on Ra.

Keywords $LaPO_4/Y_2O_3$ composite · Abrasive water jet · Garnet · Response surface method · Design optimization

✉ K. Balamurugan
kbalan2000@gmail.com

[1] Faculty of Mechanical Engineering, VFSTR University, Guntur, Andhra Pradesh 522213, India

[2] Faculty of Mechanical Engineering, Kalasalingam University, Krishnankoil 626 126, India

[3] Material Sciences and Technology Division, National Institute for Interdisciplinary Science and Technology, Council of Scientific and Industrial Research, Thiruvananthapuram 695019, India

Introduction

$LaPO_4$ and Y_2O_3 ceramic materials possess excellent thermal stability, high melting temperature, low diffusivity and least thermal expansion coefficient. Earlier studies on $LaPO_4$ reveal that this material tends to form a suitable inter-phase material and also act as a reinforcement element in the composite mixture [1]. $LaPO_4$ form a structure layer material and helps in formation of weak bond with Al_2O_3 and ZrO_2 composite. While performing the machining operation, this rare earth phosphate material forms an interfacial bond that prevents crack growth and further avoid in the deflection of crack [2]. $LaPO_4$ composite has proved to be machinable ceramic [3] and the addition of $LaPO_4$ in Al_2O_3 composites enhance in control of grain growth [4].

Among the rare earth oxides, yttrium oxide (Y_2O_3) possesses excellent properties like thermodynamic stability, ability to withstand high temperature, no phase transformation. Hence Y_2O_3 has been preferred to be an additive material to get a stabilized phase in ceramic and metal matrix composites [5]. Besides Y_2O_3 is recorded as a functional material for Eu^{3+}, Tb^{3+}, Er^{3+}, Yb^{3+}, Tm^{3+} ions in phosphorus materials and also enhance in densification of the composite with sintering temperatures [6]. Further Y_2O_3 grains will impart synergistic effects of higher hardness and strength at elevated temperature. Y_2O_3 has higher hardness compared to lanthanum phosphate material. The addition of Y_2O_3 in $LaPO_4$ will enhance the hardness of the composite which predominantly determines the machining effects of $LaPO_4$/ Y_2O_3 composite.

Water jet cutting is an industrial technology capable for cutting a wide variety of materials using high-pressure jet of water, or a mixture of water and an abrasive substance. AWJM has proven to have no heat affected zone and have the thermal free cut surface [7]. Experimental observations using AWJM on different materials over surface finish reveals that smooth

cut surface is acquired for the brittle materials with wear track and erosion type of failure on ductile materials [8]. The significant effect of JP is noticed while machining cast iron and to get smooth surface finish low levels of SOD and TS are preferred in AWJM [9]. The thickness of the materials significantly affects the performance of AWJM. The influence of TS on Ra is found to be superior over other operating parameters in AWJM [10]. The influence of abrasive flow rate and the abrasive particle size on Ra is studied with varied input parameters on aluminum materials that show diverged results with change in each parameters of AWJM [11]. The desire property of the cut material will determine the kerf angle of the cut region [12, 13]. While machining glass using different abrasives by AWJM, SOD signifies KA and MRR to greater extent [14]. The mechanism of the wear behavior of the material mainly depends on the material property and the abrasive particle [15, 16]. The impingement effect of different abrasives on eight different ceramic materials exhibits its own wear mechanism, hence it is concluded that the hard abrasives can be used to machine high toughness materials [17].

AWJM studies on Si_3N_4 show that the second-order polynomial equation of RSM fits the desire experimental values with less than 2% accuracy [18]. Earlier studies on RSM model show that JP and abrasive flow rate plays a significant role while machining AA6531 material and is stated that RSM model is a desirable method for the interpretation of the optimistic function [19]. An improved quality characteristic is obtained by using RSM with integrated Grey-RSM approach [20]. It is reported that an enviable optimistic condition on multi objective optimization was obtained in electrical discharge machining by RSM. In this study, RSM model is used to optimize the three output responses of AWJM.

The present study machines $LaPO_4/Y_2O_3$ composite prepared by aqueous sol-gel process using AWJM. The pressure comes through the nozzle (JP). The stand-off distance (SOD) is the distance between the nozzle and the work piece which is also known as the work distance. Traverse speed (TS) that denotes the cutting speed or the nozzle movement is taken as the independent parameter. MRR is measure of quantity of materials removed during the cut and the taper that formed due to the abrasives flow is measured and reported as KA and surface roughness are taken as the dependent responses. The machining and influencing effect of each independent parameter on $LaPO_4/Y_2O_3$ composite in AWJM is analyzed with the help of RSM.

Material and methods

Material preparation

$LaPO_4$ sol is used as the primary material for the preparation of $LaPO_4/Y_2O_3$ ceramic composite. To fabricate 20 g of $LaPO_4$ ceramic powder, 11.6938 g of lanthanum chloride hexa hydrate solution is mixed with 5.4 ml of 88% orthophosphoric acid with continuous stirring. The pH is brought down to ~ 2. After stirring for 2 h, 25% ammonia solution is added drop wise to flocculate the lanthanum phosphate. The precipitate formed is washed and centrifuged to remove Cl^- ions and the excess phosphate from the medium and it is then heated at a temperature of 1400 °C.

To synthesis 5 g of $LaPO_4$ + 20% Y_2O_3 nano composite, yttrium nitrate of 17 g is dissolved in minimum amount of distilled water, further 11.6938 g $LaPO_4$ sol is added under constant stirring condition. With a continuous stirring of about 3 h, the precipitation of $Y(OH)_3$ as well as flocculation of $LaPO_4$ will be slowly achieved. The pH is adjusted to 8 by addition of 25% NH_3 solution in the mixture. The precipitate obtained is then dried over water bath and further heat treated to 1400 °C to remove the moisture content. The gained powder is die compacted to a pressure of 480 MPa at ambient condition to acquire a disc shape of 36 mm × 7 mm. Finally the compressed sample is sintered to 1400 °C for 2 h. The theoretical density of the composite is calculated by rule of mixtures and is recorded as 4.95 g/cm^3. By employing Archimedes principle the experimental density is found to be 4.87 g/cm^3. The relative density of 98.4% is achieved for the developed composite.

Methods

$LaPO_4/Y_2O_3$ composite has low electrical conductivity and brittle in nature. The prepared composite is machined using AWJM of Model DIP 6D-2230. AWJM has an orifice diameter 0.25 mm with WC nozzle diameter of 0.67 mm. Garnet of 80 mesh size is used as abrasive particle. Figure 1 shows the experimental set up of AWJM.

The surface roughness tester of model SJ-411 is used to measure the surface roughness. The measurement is performed over a span of 5 mm with the measurement range and probe speed of 350 μm and 0.25 mm/s, respectively.

The high precision weighing balance of Shimadzu made of model AUX 220 is used to measure the weight of the composite material. The quantity of material removed per second is calculated using the following eq. 1.

$$MRR = \frac{(Wf - Wi) * 1000}{Dw * t} \quad (1)$$

Where, W_i—initial weight of work piece in grams before cutting, W_f—final weight of work piece in grams after cutting, D_w—density of the work piece (gm/cm^3) and t—period of trial (seconds).

Fig. 1 AWJM experimental setup

Micro structural characterization studies

SEM analysis is employed to examine the mode of failure occurred while machining the $LaPO_4/Y_2O_3$ composite at different working conditions in AWJM. The operation performed on the cut surface of the sample expels the failure mechanism and also delivers the condition of surface finish at different operated levels. ZEISS EVO series of high definition Scanning Electron Microscopy is used at a voltage level of 17.5 KV with the varied magnification.

Response surface design

Design of experiment (DOE) is a systematic method to investigate the comprehensive assessment obtained through data collection and analysis. To accrue the appropriate mathematical equations with less complexity, the second-order central composite design (CCD) is experimented. The limited number of variables in the obtained mathematical equation reduces complexity and increases the possibility of higher degree of accuracy. This action enhances the researchers to do the experimental optimization with the second-order CCD [21, 22]. The significant effect of each individual independent parameter on each dependent parameter is interrogated. The design model of L20 orthogonal array for AWJM that constitutes of 6 repetitive center level observations are done at varied time intervals. Table 1 shows the list of factors and levels. Statistical software tool of MINITAB 17 is used for the random generation of the order of the experiments. The RSM approach is used to construct the empirical equations for the three output response. The influence of each independent response and its squares are studied through the analysis of variance (ANOVA) with 95% confidential level. The quadratic equation of RSM is shown in Eq. 2.

$$Y = b_o + \sum_{i=1}^{\infty} b_i X_i + \sum_{i=1}^{\infty} b_{ii} X_i^2 + \sum_{i=1}^{\infty} \sum_{j>1}^{\infty} b_{ij} X_i X_j + \varepsilon \quad (2)$$

where, Y = response factor (MRR, KA and Ra), β_0 = co-efficient (Free Term), $\beta_{i\ =}$ linear co-efficient, β_{ii} = quadratic co-efficient, β_{ij} = interaction co-efficient and X_i, X_j = dimensionless coded independent variables.

Results and discussion

Developed empirical model of AWJM for $LaPO_4/Y_2O_3$ composite

The experimental observations of $LaPO_4/Y_2O_3$ composite for L20 orthogonal array is shown in Table 2.

ANOVA for MRR, KA and Ra for $LaPO_4/Y_2O_3$ composite are shown in Table 3. From the predicted model, the probability value (P value) for the linear equations of MRR, KA and Ra are found to be zero. Lower the P value reply and the linear dependency of all independent variables over the output responses. The lack of fit of P value for the MRR, KA and Ra are identified to be significant because the achieved P values through the regression are found to be lesser than 0.05%.

Table 4 shows the estimated regression co-efficient for MRR, KA and Ra. The significant relation exists between the co-efficient can be identified through smaller P value and either by larger T value [23]. For MRR model, all the three linear models of the independent parameter have P value as zero. This shows the influence of each independent parameter over the output responses. To identify the maximum level of influence among the independent parameters, the T value is taken into consideration. The higher T value gives a significant effect on the dependent variables. Through T value

Table 1 Selected factor and levels

S.No	Independent variables	Symbols	Levels			Units
			−1	0	1	
1	Jet pressure	JP	220	240	260	bar
2	Stand-off-distance	SOD	1	2	3	mm
3	Traverse speed	TS	20	30	40	mm/s

Table 2 The experimental observations of $LaPO_4/Y_2O_3$ composite

Test numbers	Independent parameters			Dependent responses		
	JP (bar)	SOD (mm)	TS (mm/min)	MRR (g/s)	KA (deg)	Ra (μm)
1	0	0	0	0.02984	0.258	3.608
2	1	0	0	0.02419	0.205	4.112
3	0	0	1	0.02399	0.215	4.134
4	− 1	0	− 1	0.02497	0.159	3.426
5	1	1	1	0.02511	0.192	5.142
6	0	0	0	0.03515	0.165	3.594
7	− 1	− 1	− 1	0.02493	0.195	1.664
8	0	− 1	0	0.02834	0.214	2.635
9	1	− 1	1	0.02342	0.162	3.982
10	0	0	− 1	0.02707	0.198	3.212
11	0	0	0	0.02908	0.152	3.706
12	0	− 1	1	0.02224	0.142	2.482
13	0	0	0	0.02496	0.169	3.682
14	0	0	0	0.02378	0.172	3.645
15	1	− 1	− 1	0.03006	0.226	3.141
16	− 1	1	1	0.01941	0.143	4.384
17	1	1	− 1	0.02469	0.163	4.526
18	0	0	0	0.03127	0.102	3.713
19	0	0	0	0.02271	0.184	3.645
20	0	1	0	0.02433	0.172	4.464

observation from the regression table, the influencing effect for MRR can be stated in the decreasing order by the linear JP, followed by linear SOD and linear TS. However for MRR, the three independent parameters show almost equal contributions and a least effect is caused by quadratic TS. The interaction between JP*TS have found to have a significant effect on MRR.

From the predicted model for KA, it is identified that almost all the three independent parameters have an equal contribution on output response. *P* value for the three linear independent parameters is zero, by considering *T* value from the regression table, the level of influencing effects can be ordered from high to low as linear JP, followed by SOD and TS. Quadratic JP and the interaction between JP*TS and SOD*TS had found to produce a least significant effect over KA.

Similar observations like other two dependent variables (MRR and KA) models are found for Ra. Based on *T* value, the significant effects for Ra are rated from high to low as; linear SOD, followed by JP and TS. The rate of influence of JP and SOD are found to be the same and produce the similar effect with change in levels irrespective of TS, while machining this new composite. Quadratic TS and the interaction between JP*TS and SOD*TS had found to have a least significant effect on Ra. It is also observed that other interaction parameters had contributed a very least effect on Ra.

The percentage of residual square (R^2) for MRR, KA and Ra are found to be greater than 95%. Hence, the generated model of MRR, KA and Ra are said to be significant. The empirical equations for MRR, KA and Ra are shown in Eqs. (3), (4) and (5), respectively.

$$\begin{aligned}\mathrm{MRR} = {} & 0.198 - 0.00148\ \mathrm{JP} - 0.0087\ \mathrm{SOD} - 0.0004\ \mathrm{TS} \\ & + 0.000003\ \mathrm{JP}^{*}\mathrm{JP} + 0.001428\ \mathrm{SOD}^{*}\mathrm{SOD} \\ & + 0.000019\ \mathrm{JP}^{*}\mathrm{SOD} + 0.000037\ \mathrm{SOD}^{*}\mathrm{TS}\end{aligned} \quad (3)$$

$$\begin{aligned}\mathrm{KA} = {} & -0.769 + 0.0057\ \mathrm{JP} + 0.072\ \mathrm{SOD} - 0.0039\ \mathrm{TS} \\ & + 0.00805\ \mathrm{SOD}^{*}\mathrm{SOD} + 0.000060\ \mathrm{TS}^{*}\mathrm{TS} \\ & - 0.000306\ \mathrm{JP}^{*}\mathrm{SOD} - 0.000163\ \mathrm{SOD}^{*}\mathrm{TS}\end{aligned} \quad (4)$$

$$\begin{aligned}\mathrm{Ra} = {} & 13.3 - 0.161\ \mathrm{JP} + 3.257\ \mathrm{SOD} + 0.130\ \mathrm{TS} \\ & + 0.000432\ \mathrm{JP}^{*}\mathrm{JP} - 0.187\ \mathrm{SOD}^{*}\mathrm{SOD} \\ & - 0.00698\ \mathrm{JP}^{*}\mathrm{SOD} - 0.000201\ \mathrm{JP}^{*}\mathrm{TS} \\ & - 0.00104\ \mathrm{SOD}^{*}\mathrm{TS}\end{aligned} \quad (5)$$

Effect of control parameters of MRR

Three-dimensional (3-D) surface plot of control response (dependent parameter) for MRR is shown in the Fig. 2. Through Figure (a), it is observed that MRR increases with the increase in levels of JP and SOD. High pressure water beam accelerates the abrasive particles and these abrasives hit within

Table 3 ANOVA of MRR, KA, and Ra

Analysis of variance of MRR					
Source	DF	Adj SS	Adj MS	*F* value	*P* value
Model	9	0.000251	0.000028	75.95	0.000
Linear	3	0.000217	0.000072	197.18	0.000
JP	1	0.000100	0.000100	271.90	0.000
SOD	1	0.000067	0.000067	183.50	0.000
TS	1	0.000050	0.000050	136.14	0.000
Square	3	0.000032	0.000011	28.64	0.000
JP*JP	1	0.000005	0.000005	13.21	0.005
SOD*SOD	1	0.000006	0.000006	15.27	0.003
TS*TS	1	0.000000	0.000000	0.03	0.856
2-way interaction	3	0.000002	0.000001	2.02	0.175
JP*SOD	1	0.000001	0.000001	3.06	0.111
JP*TS	1	0.000000	0.000000	0.06	0.811
SOD*TS	1	0.000001	0.000001	2.94	0.117
Error	10	0.000004	0.000000		
Lack-of-fit	5	0.000002	0.000000	1.59	0.312
Pure error	5	0.000001	0.000000		
Total	19	0.000255			
R^2 = 98.56%, adjacent R^2 = 97.26%					
Analysis of variance of KA					
Source	DF	Adj SS	Adj MS	*F* value	*P* value
Model	9	0.022173	0.002464	26.09	0.000
Linear	3	0.021230	0.007077	74.96	0.000
JP	1	0.008122	0.008122	86.03	0.000
SOD	1	0.006656	0.006656	70.50	0.000
TS	1	0.006452	0.006452	68.34	0.000
Square	3	0.000566	0.000189	2.00	0.178
JP*JP	1	0.000033	0.000033	0.35	0.569
SOD*SOD	1	0.000178	0.000178	1.89	0.200
TS*TS	1	0.000101	0.000101	1.06	0.326
2-way interaction	3	0.000376	0.000125	1.33	0.319
JP*SOD	1	0.000300	0.000300	3.18	0.105
JP*TS	1	0.000055	0.000055	0.58	0.462
SOD*TS	1	0.000021	0.000021	0.22	0.646
Error	10	0.000944	0.000094		
Lack-of-fit	5	0.000351	0.000070	0.59	0.710
Pure error	5	0.000593	0.000119		
Total	19	0.023117			
R^2 = 95.92%, adjacent R^2 = 92.24%					
Analysis of variance of Ra					
Source	DF	Adj SS	Adj MS	*F* value	*P* value
Model	9	11.2584	1.25093	36.23	0.000
Linear	3	10.9336	3.64454	105.55	0.000
JP	1	2.7447	2.74471	79.49	0.000
SOD	1	6.4642	6.46416	187.22	0.000
TS	1	1.7247	1.72474	49.95	0.000
Square	3	0.1551	0.05169	1.50	0.274
JP*JP	1	0.0822	0.08222	2.38	0.154
SOD*SOD	1	0.0957	0.09574	2.77	0.127
TS*TS	1	0.0109	0.01095	0.32	0.586
2-way interaction	3	0.1697	0.05657	1.64	0.242
JP*SOD	1	0.1560	0.15596	4.52	0.059
JP*TS	1	0.0129	0.01288	0.37	0.555
SOD*TS	1	0.0009	0.00086	0.02	0.878
Error	10	0.3453	0.03453		
Lack-of-fit	5	0.3354	0.06707	33.82	0.001
Pure error	5	0.0099	0.00198		
Total	19	11.6037			
R^2 = 97.02%, adjacent R^2 = 94.35%					

themselves, also the pressure variation creates a wider jet beam before it hits the top surface of the sample. SOD has greater influence on increase in the width of the jet beam. At low JP, the rate of increase of MRR is low with respect to SOD. However, from the plot it is observed that the optimum operating conditions for MRR is expected to lie within the range of acceptance. From Figure (b), it is observed that MRR of $LaPO_4/Y_2O_3$ reduces on increase in TS, where the change in levels of JP creates an adverse effect on machining. High TS limits the machining time and creates surface

Table 4 Estimated regression co-efficient of MRR, KA, and Ra

Estimated regression co-efficient of MRR				
Term	Coef	SE Coef	*T* value	*P* value
Constant	0.024565	0.000208	117.91	0.000
JP	0.003160	0.000192	16.49	0.000
SOD	0.002596	0.000192	13.55	0.000
TS	− 0.002236	0.000192	− 11.67	0.000
JP*JP	0.001328	0.000365	3.63	0.005
SOD*SOD	0.001428	0.000365	3.91	0.003
TS*TS	0.000068	0.000365	0.19	0.856
JP*SOD	0.000375	0.000214	1.75	0.111
JP*TS	0.000053	0.000214	0.25	0.811
SOD*TS	0.000367	0.000214	1.72	0.117
Estimated regression co-efficient of KA				
Term	Coef	SE Coef	*T* value	*P* value
Constant	0.17408	0.00334	52.12	0.000
JP	0.02850	0.00307	9.28	0.000
SOD	0.02580	0.00307	8.40	0.000
TS	0.02540	0.00307	8.27	0.000
JP*JP	− 0.00345	0.00586	− 0.59	0.569
SOD*SOD	0.00805	0.00586	1.37	0.200
TS*TS	0.00605	0.00586	1.03	0.326
JP*SOD	− 0.00613	0.00344	− 1.78	0.105
JP*TS	0.00263	0.00344	0.76	0.462
SOD*TS	− 0.00162	0.00344	− 0.47	0.646
Estimated regression co-efficient of Ra				
Term	Coef	SE Coef	*T* value	*P* value
Constant	3.6831	0.0639	57.66	0.000
JP	0.5239	0.0588	8.92	0.000
SOD	0.8040	0.0588	13.68	0.000
TS	0.4153	0.0588	7.07	0.000
JP*JP	0.173	0.112	1.54	0.154
SOD*SOD	− 0.187	0.112	− 1.67	0.127
TS*TS	− 0.063	0.112	− 0.56	0.586
JP*SOD	− 0.1396	0.0657	− 2.13	0.059
JP*TS	− 0.0401	0.0657	− 0.61	0.555
SOD*TS	− 0.0104	0.0657	− 0.16	0.878

waviness on the rough cut region. The surface plotted between MRR and SOD vs TS is shown in Figure (c) which exhibits a similar effect as in Figure (b). The influence of SOD and TS on MRR is linear and the maximum point for the experimental region will be located outside the plotted region. The predicted working condition of independent variable is suggested to be JP = 220 bar, SOD = 1.10 mm and TS = 40 mm/s. The RSM model gives a new level for SOD to acquire a minimum MRR.

Effect of control parameters on KA

The 3-D surface plot of independent parameters for KA is shown in Fig. 3. From Figure (a), a slight increase with decreasing trend for KA is observed with the progressive increase of JP and SOD. Figure (b) shows a linear change in KA with increase in JP and TS, respectively. However the effect of TS is recorded to be superior to JP, while machining $LaPO_4/Y_2O_3$ composite. Rapid movement of the nozzle irrespective of JP creates a narrow cut in the bottom region. Figure (c) of KA shows a slight decrease and progressive rise with change in SOD. The progressive increase on TS is recorded. From the result, it is observed that the influence of JP and TS are high irrespective of SOD. To perform a cutting operation in AWJM for this composite, a minimum level of JP and TS is recommended because the optimal point is expected to be on the outside of the plotted region. Increase in TS irrespective of JP reduces the high accelerated abrasives flow in the bottom region of the composite. This action reduces the

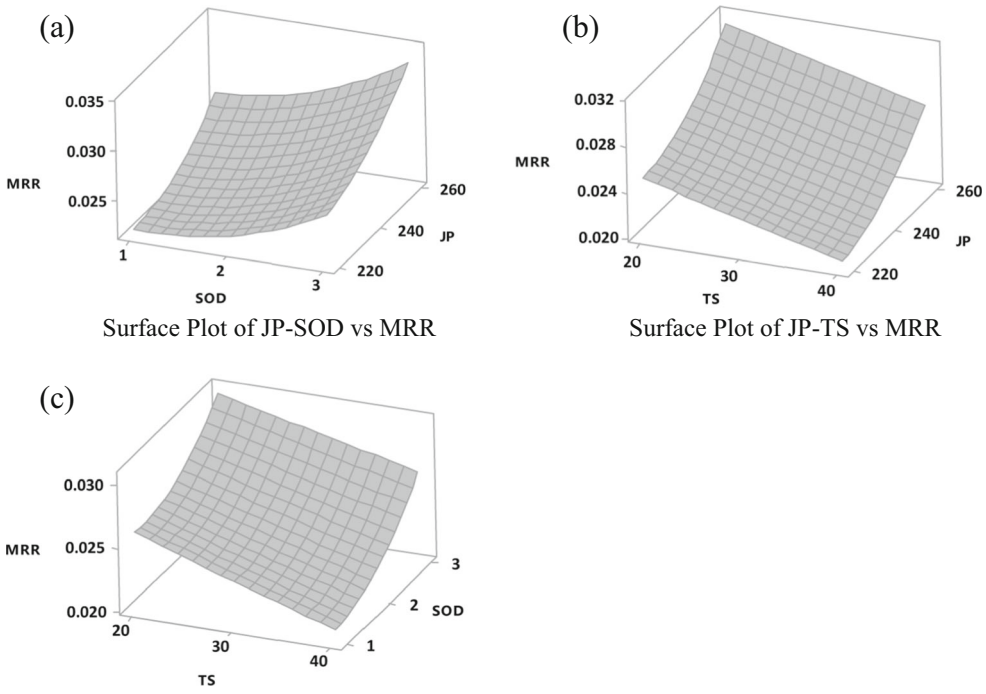

Fig. 2 Surface plots of the combined effects of the independent parameters on MRR

MRR and produces a tapered surface that deliberately creates an increase in kerf angle. The optimum working condition to acquire minimum KA is predicted to be JP = 220 bar, SOD = 1 mm and TS = 20 mm/s.

Effect of control parameters on Ra

The 3-D response surface plot of Ra from the predicted model is shown in Fig. 4. The combined effect of JP and SOD with

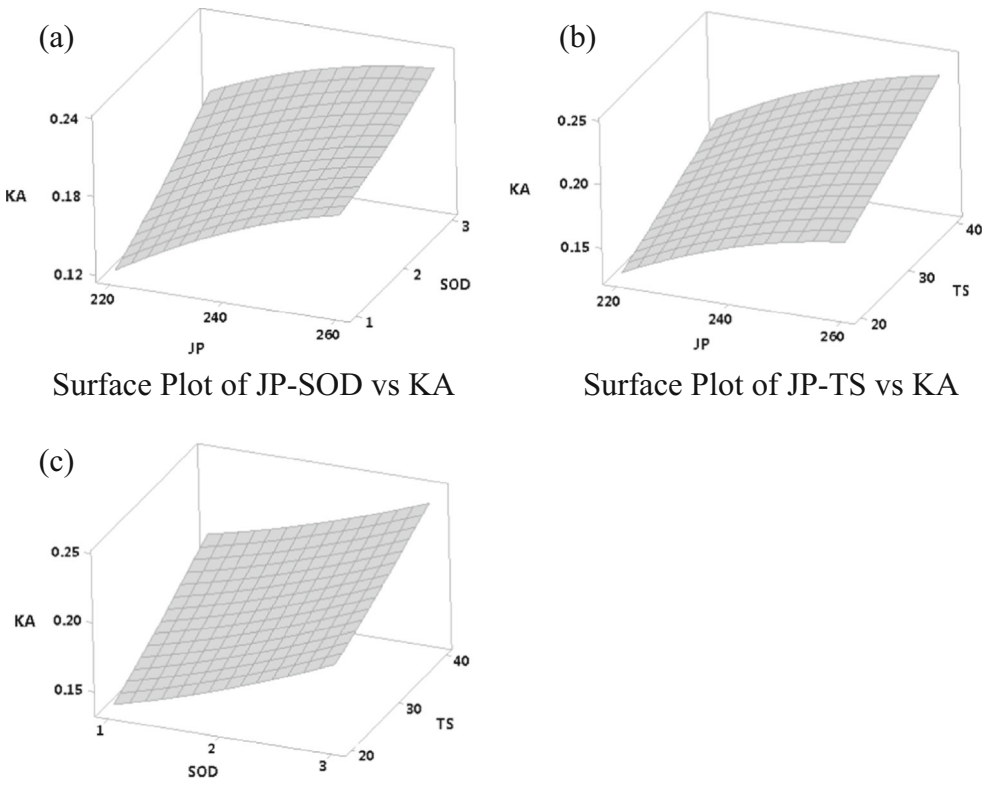

Fig. 3 Surface plots of the combined effects of the independent parameters on KA

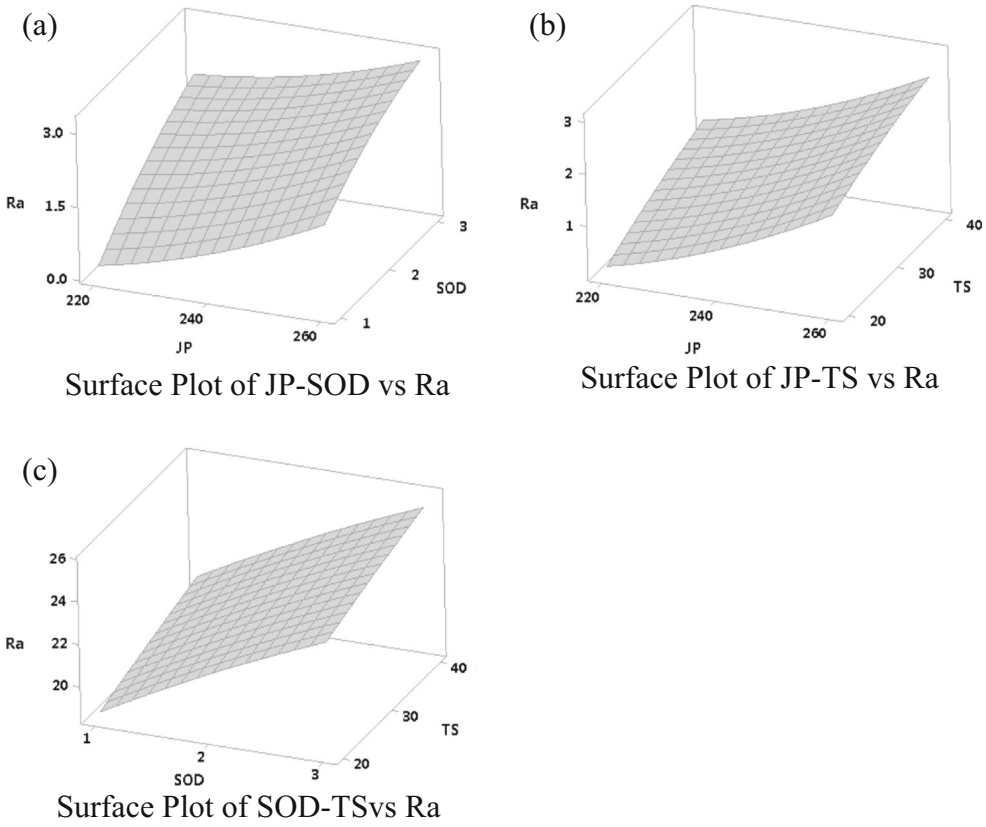

Fig. 4 Surface plots of the combined effects of the independent parameters on Ra

Ra is shown in Figure (a). The contribution of these two parameters on Ra is found to exhibit a saddle point at some point in the plotted region. This point is an inflection point between a relative maximum and a relative minimum. To obtain a maximum or minimum response to a studied system, the saddle point coordinates do not serve as optimal values. Again, it is possible to find the optimum region through visual inspection of the surfaces. The optimal working condition might be occurred at some different operating levels.

Figure (b) shows the combined regression surface plot of JP and TS for Ra and the effects of these parameters produce a similar effect as JP and SOD on Ra. However, the influencing effect of TS is high with change in JP. Figure (c) shows the parametric effect of SOD and TS on Ra. The higher the operating levels of TS larger the value of Ra. Through the obtained surface plot, it became possible to predict the optimal condition. From Figure (a–c), it could be confirmed that all the three independent parameters have a significant effect on Ra. However the rate of change of the three influencing factors on Ra increases with increase in operating levels. The acceptable level of Ra is achieved at low level operating conditions of JP = 220 bar, SOD = 1 mm and TS = 20 mm/s in AWJM.

Sub-microscopic analysis

SEM image on the cut surface shows the presence of both transgranular and intergranular fractures and is shown in Fig. 5. Figure (a) shows the presence of rupture region all over

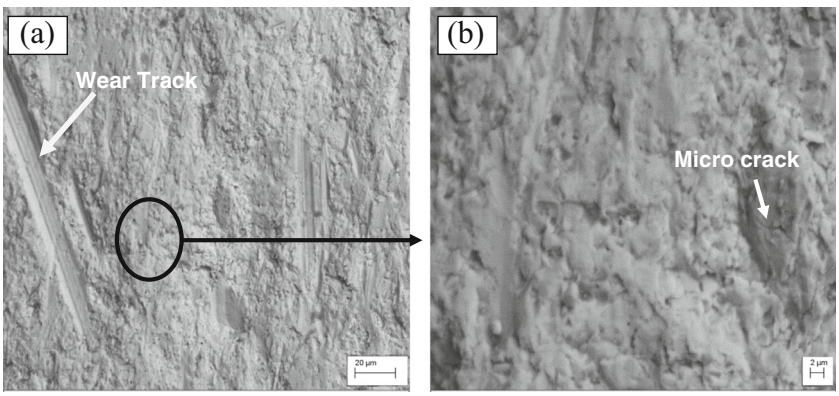

Fig. 5 SEM micrograph of AWJM cut region of $LaPO_4/Y_2O_3$ composite

the cut surface with dimples and micro crack confirms that the machined surface is plastic deformation surface. The micro level wear track and scar that are created by the impinged of the abrasives are clearly visible. As the high accelerated abrasive hits the composite surface and when it expels out after machining, it collides with new abrasives and creates wear track in a random order. The wear track demonstrates the abrasive flow direction. On closer observation, it is noticed that the micro level crack propagated along the grains and the grain boundary and is shown in Figure (b). Micro cracks are formed due to the simultaneous heating and cooling effects on the cut surface. As the hard abrasives impinge the composite, there is a raise in temperature. Since the working medium is water, cooling takes place at the instant create micro cracks.

The hard abrasives tear the composite and create the peaks and valley regions on the cut surface. The high accelerated abrasive tends to break the bond energy between the elements in the composite and hence the machining is done by erosion. The mechanism behind the removal of materials confirms the ease of machinability of the composite material by AWJM.

The microscopic observation clearly delivers that the effect of high traverse speed will significantly enhance the surface property of the composite. Further it is noticed that in AWJM irrespective of TS, even at all level operating conditions an acceptable level of Ra is obtained with the measure of 1.664, 2.635 and 2.482 μm. The consequences of increase in the width of the water beam tend to increase the machined area of the top surface of the composite. Owing to the increase in TS, a smaller opening is observed at the bottom of the composite. This leads to form the striation on the bottom region of the cut surface, which substantially affects Ra of the composite material.

Conclusions

This study evaluates the influences and the significant effects of the three independent variables (JP, SOD and TS) of AWJM on $LaPO_4/Y_2O_3$ composite on use of garnet as abrasive and the conclusions drawn as follows:

- By RSM model, the correlation exists between the JP, SOD and TS of AWJM on $LaPO_4$ + 20%Y_2O_3 that are examined. From the obtained results it can be stated that all the three considered independent parameters had played a significant role to the output responses.
- From ANOVA table, it is estimated that the three independent parameters affect the MRR in the equal proportion, however based on their influencing effect it is in the following decreasing order; linear JP, SOD and TS. A least significant effect is observed by Quadratic TS. To the interaction part a least effect of JP*TS is recorded.
- By ANOVA table, the significant effect of three independent parameters on KA shows equal contribution. Based on the influencing factors, the order is that JP is followed by SOD and TS. Among the other determinant factors, quadratic JP and the interaction between JP*TS and SOD*TS have a least significant effect.
- By ANOVA of Ra, it is stated that SOD has the most significant role, followed by JP and TS. Further, quadratic TS and interaction between JP*TS and SOD*TS has a least influencing effect.
- SEM analysis on the machined surface reveals the presence of micro wear cracks and wear track over the regions. Further the presence of rupture region with dimples confirm the plastic deformation cut surface. Peeling off and deep wear track explain the ease of machinability of the functional composite by other conventional machining practices.
- The predicted optimization conditions for each output responses of $LaPO_4/Y_2O_3$ composite in AWJM are estimated to be; for MRR is JP = 220 bar, SOD = 1.10 mm and TS = 40 mm/s, for KA is JP = 220 bar, SOD = 1 mm and TS = 20 mm/s and for Ra JP = 220 bar, SOD = 1 mm and TS = 20 mm/s

Acknowledgements The authors feel grateful to the DST-FIST sponsored Advance Machining and measurement lab of Kalasalingam University for their support to finish this work.

References

1. Marshall, D.B., Morgan, P.E.D., Housley, R.M., Cheung, J.T.: High-temperature stability of the Al_2O_3–$LaPO_4$ system. J. Am. Ceram. Soc. **81**, 951–956 (1998)
2. Majeed, M.A., Vijayaraghavan, L., Malhotra, S.K., Krishnamurthy, R.: Ultrasonic machining of $Al_2O_3/LaPO_4$ composites. J. Mach. Tools Manuf. **48**, 40–46 (2008)
3. Davis, J.B., Marshall, D.B., Morgan, P.E.D.: Monazite-containing oxide/oxide composites. J. Eur. Ceram. Soc. **20**, 583–587 (2000)
4. Wang, R., Pan, W., Chen, J., Jiang, M., Luo, Y., Fang, M.: Properties and microstructure of machinable $Al_2O_3/LaPO_4$ ceramic composites. Ceram. Int. **29**, 19–25 (2003)
5. Zhu, X., Lu, Z., Wei, B., Huang, X., Zhang, Y., Su, W.: A symmetrical solid oxide fuel cell prepared by dry-pressing and impregnating methods. J. Power Sources. **196**, 729–733 (2011)
6. Lloyd, I.K.: Advances in electro ceramic materials II. Ceram. Trans. **221**, 115–124 (2010)
7. Zhang, S., Wu, Y., Wang, Y.: A review on abrasive waterjet and wire electrical discharge machining–high speeds. Open Mech. Eng. J. **5**, 178–185 (2011)
8. Zhao, W., Guo, C.: Topography and microstructure of the cutting surface machined with abrasive waterjet. J. Adv. Manuf. Technol. **73**, 941–947 (2014)
9. Selvan, M.,.C.,.P., Raju, N.M.S.: Analysis of surface roughness in abrasive waterjet cutting of cast iron. Int. J. Sci. Environ. Technol. **1**, 174–182 (2012)

10. Derzija, B.H., Ahmet, C., Muhamed, M., Almina, D.: Experimental study on surface roughness in abrasive water jet cutting. Procedia Eng. **100**, 394–399 (2015)
11. Babu, N.M., Fernando, A.G.A., Muthukrishnan, N.: Analysis on surface roughness in abrasive water jet machining of aluminium. Prog. Ind. Ecol. **9**, 200–206 (2015)
12. Alberd, A., Artaza, T., Suarez, A., Rivero, A., Girot, F.: An experimental study on abrasive waterjet cutting of CFRP/Ti_6Al_4V stacks for drilling operations. J. Adv. Manuf. Technol. **86**, 691–704 (2015)
13. Hocheng, H., Chang, K.R.: Material removal analysis in abrasive waterjet cutting of ceramic plates. J. Mater. Process. Technol. **40**, 287–304 (1994)
14. Khan, A.A., Haque, M.M.: Performance of different abrasive materials during abrasive water jet machining of glass. J. Mater. Process. Technol. **191**, 404–397 (2007)
15. Ren, X., Peng, Z., Hu, Y., Wang, C., Fu, Z., Yue, W., Qi, L., Miao, H.: Abrasive wear behavior of TiCN cermets under water-based slurries with different abrasives. Tribol. Int. **66**, 35–43 (2013)
16. Akkurt, A., Kulekci, M.K., Seker, U., Ercan, F.: Effect of feed rate on surface roughness in abrasive waterjet cutting applications. J. Mater. Process. Technol. **147**, 389–396 (2004)
17. Yamamoto, T., Olsson, M., Hongmark, S.: Three-body abrasive wear of ceramic materials. Wear. **74**, 21–31 (1994)
18. Ghosh, D., Doloi, B., Das, P.K.: Parametric analysis and optimisation on abrasive water jet cutting of silicon nitride ceramics. J. Precis. Technol. **5**(3/4), 294–311 (2015)
19. Babu, N.M., Muthukrishnan, N.: Investigation on surface roughness in abrasive water jet machining by the response surface method. J. Mater. Manuf. Process. **29**, 1422–8 (2014)
20. Adalarasan, R., Santhanakumar, M., Rajmohan, M.: Application of Grey Taguchi-based response surface methodology (GT-RSM) for optimizing the plasma arc cutting parameters of 304L stainless steel. J. Adv. Manuf. Technol. **78**, 1161–1170 (2015)
21. Bezerra, M.A., Santelli, R.E., Oliveira, E.P., Villar, L.S., Escaleira, L.A.: Response surface methodology (RSM) as a tool for optimization in analytical chemistry. Talanta. **76**, 965–977 (2008)
22. Agarwal, S., Tyagi, I., Gupta, V.K., Bagheri, A.R., Ghaedi, M., Asfaram, A., Hajati, S., Bazrafshan, A.A.: Rapid adsorption of ternary dye pollutants onto copper (I) oxide null nano particle loaded on activated carbon: experimental optimization via null response surface methodology. J. Environ. Chem. Eng. **4**, 1769–1779 (2016)
23. Noordin, M.Y., Venkatesh, V.C., Sharif, S., Elting, S., Abdullah, A.: Application of response surface methodology in describing the performance of coated carbide tools when turning AISI1045 steel. J. Mater. Process Technol. **145**, 46–58 (2004)